

The Impact of Covid-19 Pandemic on Land Surface Temperature in Yogyakarta Urban Agglomeration

Erlyna Nour Arrofiqoh ^{1*}, Devika Ayu Setyaningrum ²

^{1,2} Teknologi Survei dan Pemetaan Dasar, Departemen Teknologi Kebumihan, Sekolah Vokasi,
Universitas Gadjah Mada, Indonesia

*Corresponding author e-mail: erlyna_na@mail.ugm.ac.id

Received: January 16, 2021

Accepted: July 08, 2021

Published: July 10, 2021

Copyright © 2021 by author(s) and
Scientific Research Publishing Inc.

Open Access



Abstract

Since the end of 2019, the world has been surprised by Corona Virus (COVID-19) pandemic. The first case of COVID-19 in Indonesia was reported in March 2020. The Indonesian policymakers have announced to limit social interaction by applying physical distancing and appealed to stay at home to slow the spread of COVID-19. Yogyakarta city is known as a tourism city and student city also affected by the presence of COVID-19. Many tourist destinations, schools, colleges, institutions, companies, and industries not operating as usually because people have been appealed to work and study at home. Less outdoor activities caused the vehicle emission in the street is rarely. This condition makes the temperature is cooler. This paper aimed to analyze the impact of the COVID-19 pandemic on the land surface temperature. Landsat 8 satellite data has been used to show the changes in LST before the pandemic, during a pandemic, and after the new normal. The results showed that during the emergence of the COVID-19 pandemic with reducing outdoor activities, the LST was lower than before the pandemic. Whereas after the new normal, the LST was increased.

Keywords: *Land surface temperature, COVID-19, physical distancing, New Normal, Yogyakarta Urban Agglomeration*

1. Introduction

Yogyakarta city runs into rapid urban growth dan development over the past decades. This urban expansion which called with urban agglomeration area has led to changes in land cover. The built-up urban area is wider than the vegetation cover. The replacement of vegetation and evaporating surface with impervious surface induces the surface temperature of urbanized areas is getting warmer because the impervious surfaces absorb the radiation and emit heat to the surrounding (Feng et al., 2019; Pal and Ziaul, 2017; Sekertekin and Zadbagher, 2021). This impervious surface is mainly contributed by materials like concrete, bricks, tiles, and asphalt for buildings, roads, and parking areas (Mathew et al., 2016).

The heat comes from roads by friction from tires and engine exhaust. Besides vehicular emission and combustions, the heat and emission from the industrial sector and power plant region also influence the land surface temperature (LST) in the city (Phelan et al., 2015). The phenomenon caused by the warmer temperature of urban areas compared with the surrounding area or a nearby rural

environment called with UHI-Urban Heat Island (Miles and Esau, 2017; Wang et al., 2020)

Starting at the end of 2019, it has been a year that we have survived the Corona Virus Pandemic. Corona Virus Diseases (COVID-19) was firstly identified in Wuhan, China, and has been infected many people all over the world (Kong et al., 2020). The virus spreads fast and the first case of COVID-19 in Indonesia was reported on March 2020. The Indonesian policymakers have announced to limit social interaction by applying physical distancing and appealed to stay at home to slow the spread of COVID-19.

Yogyakarta city is known as a tourism city and student city also affected by the presence of COVID-19. Many tourist destinations, schools, colleges, institutions, companies, and industries not operating as usual because people have been appealed to work and study at home. Limitations on outdoor activities reduce the transport mobilization, both private and public transportation. The emission of gas and combustion smoke in the roads is decreased. This condition makes the temperature is

cooler. and appealed to stay at home to slow the spread of COVID-19.

In the beginning, on July 2020, D. I. Yogyakarta applied a new normal policy. People do not always live in quarantine, people must start activities in various sectors by strictly implementing health protocols so there is harmony and vigilance in the prevention and handling of Covid-19. A number of scientists predict the Covid-19 pandemic can last a long time because the vaccine for Covid-19 has not been found. Under these conditions, the Regional Government must implement a new pattern of work that is adjusted to the character of the coronavirus. The new normal policy makes outdoor activities increase. This is possible will cause changes in air quality which can affect surface temperatures.

This paper aimed to analyze the effect of the COVID-19 pandemic on the land surface temperature (LST) over Yogyakarta Urban Agglomeration. Thermal remote sensing data acquired by Landsat 8 satellite has been used to show the changes in LST before the pandemic, during the pandemic, and after new normal changes in air quality which can affect surface temperatures.

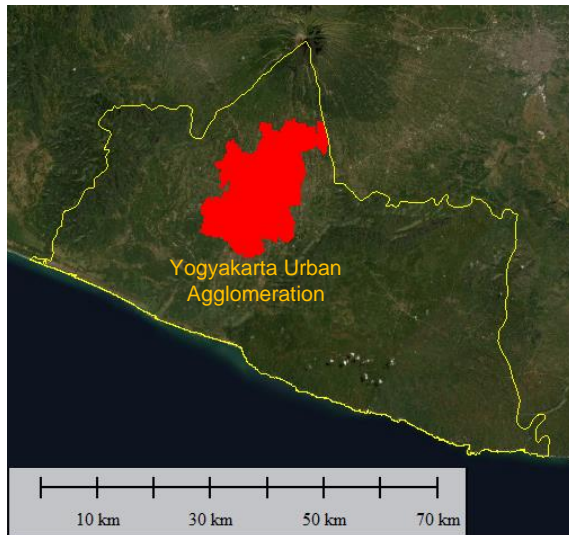


Fig. 1. Map of the study area

2. Materials and Methods

2.1 Data

This study uses Landsat 8 OLI/TIRS from Earth Explorer website (earthexplorer.usgs.gov). The band needed for this research is thermal infrared band (band 10 TIRS), red visible band (band 4) and near-infrared band (band 5). This research also uses administrative boundaries of Yogyakarta Urban Agglomeration. This table 1 shows the details of the acquisition date is used in this study.

Table 1. Data of the satellite images

date	description
12 – 08 – 2019	Before pandemic
10 – 05 – 2020	During pandemic
30 – 08 – 2020	After new normal

2.2 Data Processing

The data processing method is illustrated by the flow chart in Figure 2. This process using open-source software QGIS. The beginning to processed LST starts from inputting the thermal infrared band 10 (TIRS band) of Landsat 8 satellite image from three different date acquisitions (before the pandemic, during the pandemic, and after new normal). Then calculate TOA (Top of atmospheric) spectral radiance. The thermal infrared radiation ($L\lambda$) can be given by (Maithani et al., 2020):

$$L\lambda = M_L * Q_{cal} + A_L \quad (1)$$

where M_L represents the band-specific multiplicative rescaling factor, Q_{cal} is the DN value for Band 10 image, A_L is the band-specific additive rescaling factor. The information of M_L and A_L can be acquired from image metadata file (see in Table 2) .

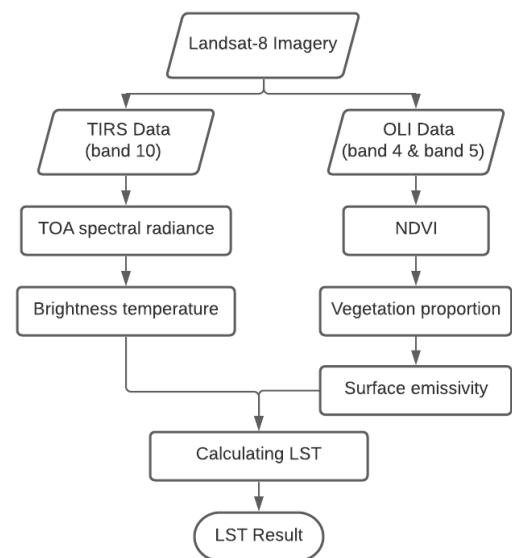


Fig. 2. LST processing flowchart

The TIRS band data must be converted from spectral radiance to brightness temperature (BT) using the thermal constants. The formula for determining BT as follows (Ndossi and Avdan, 2016):

$$BT = \frac{K_2}{\ln [(K_1/L\lambda)+1]} - 273.15 \quad (2)$$

where K_1 and K_2 stand for the band-specific thermal conversion constants from the metadata file. The radiant temperature estimated in Kelvin scale and converted into degree Celsius scale by subtracting 273.15.

Table 2. Metadata of the satellite images

Units	Value
Thermal constant (band 10)	K_1 : 774.8853
	K_2 : 1321.0789
Rescaling factor (band 10)	M_L : 0,0003342
	A_L : 0.1

The next step is to calculate Normal Difference Vegetation Index (NDVI). NDVI is one of the methods

for measuring the level of greenness vegetation by comparing between spectral near-infrared band with red visible band. NDVI can be used to estimated general vegetation condition. The formula for NDVI as in this equation (Logan et al., 2020) :

$$NDVI = \frac{NIR-R}{NIR+R} \quad (3)$$

where NIR stands for near-infrared band (Band 5) and R represents the red band (Band 4). The proportion of vegetation was calculated based on the NDVI threshold value. PV is a ratio of the vertical projection area of vegetation (leaves, stalks, and branches) on the ground to the total vegetation area (Neinavaz et al., 2020). The proportion of vegetation (P_v) calculated using the following formula (Srivastava et al., 2014; Bendib et al., 2017):

$$P_v = \left(\frac{NDVI - NDVI_{min}}{NDVI_{max} - NDVI_{min}} \right)^2 \quad (4)$$

where P_v = Proportion of vegetation, NDVI = Normalized Difference Vegetation Index, NDVI_{max} = maximum value of NDVI = NDVI_v (NDVI Vegetation), and NDVI_{min} = minimum value of NDVI = NDVI_s (NDVI Soil). Emissivity is the ability of an object to emit radiation (Planck's law). Land surface emissivity (ε_λ) is an element to estimate LST. Land surface emissivity is calculated as suggested in (Avdan and Jovanovska, 2016) :

$$\varepsilon_\lambda = \varepsilon_{v\lambda}P_v + \varepsilon_{s\lambda}(1 - P_v) + C_\lambda \quad (5)$$

where ε_v and ε_s are the vegetation and soil emissivities, C represents the surface roughness (C = 0 for homogenous and flat surfaces). The condition can be represented with the following equation (Yu et al., 2014) :

$$\varepsilon_\lambda = \begin{cases} \varepsilon_{s\lambda}, & NDVI < NDVI_s \\ \varepsilon_{v\lambda}P_v + \varepsilon_{s\lambda}(1 - P_v) + C, & NDVI_s \leq NDVI \leq NDVI_v \\ \varepsilon_{v\lambda} + C, & NDVI > NDVI_v \end{cases} \quad (6)$$

The last step is the retrieving LST. LST has been calculated using at-sensor brightness temperature (BT) and land surface emissivity (ε_λ). LST is computed as follows (Sahani et al., 2020) :

$$LST = \frac{BT}{[1 + (\lambda \cdot \frac{BT}{\rho}) \cdot \ln \varepsilon_\lambda]} \quad (7)$$

where LST in Celsius (°C), BT is at-sensor BT (°C), λ is the wavelength of emitted radiance (for which the peak response and the average of the limiting wavelength, ε_λ is the emissivity, and ρ acquired from Planks equation:

$$\rho = h \frac{c}{\sigma} = 1.438 \times 10^{-2} mK \quad (8)$$

where σ is the Boltzmann constant (1.38 × 10⁻²³ J/K), h is Planck's constant (6.626 × 10⁻³⁴ J s), and c is the velocity of light (2.998 × 10⁸ m/s).

3. Result and Discussion

In this study, the surface temperature maps for Yogyakarta Urban Agglomeration have been produced using Landsat 8 OLI/TIRS sensors and processed with the LST algorithm. The result of the LST map is shown in Figure 3, Figure 4, and Figure 5. These figures of temperature map show a comparison of the surface temperature over Yogyakarta Urban Agglomeration before pandemic (August 2019), during pandemic (May 2020), and after new normal (August 2020). From that figures can indicate that temperature decreases due to the COVID-19 pandemic and increased again after the new normal.

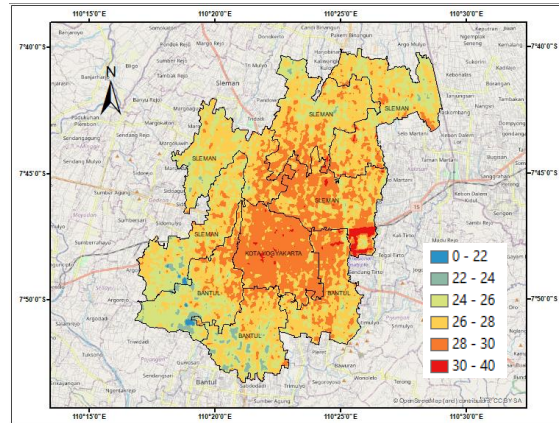


Fig. 3. Temperature map before pandemic (August 2019)

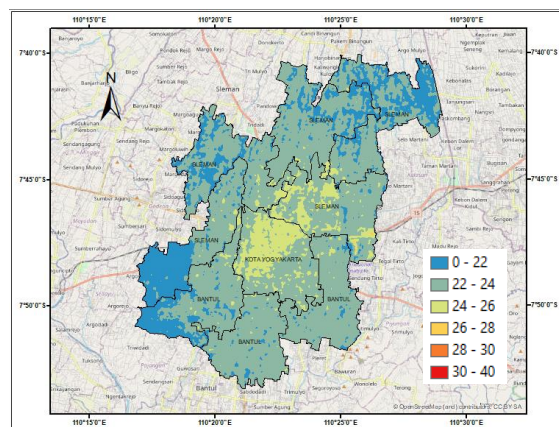


Fig. 4. Temperature map during pandemic (May 2020)

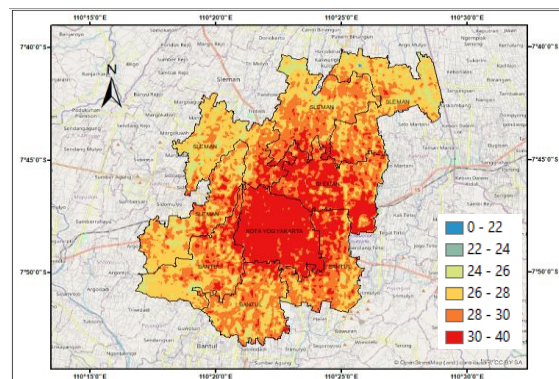


Fig. 5. Temperature map after new normal (August 2020)

The information regarding decreasing of LST due to COVID-19 pandemic in Yogyakarta Urban Agglomeration is shown in Table 3.

Table 3. Comparison of temperature parameters in Yogyakarta Urban Agglomeration

Category	Before pandemic	During pandemic	After new normal
Min Temp.	18.14	6.38	21.40
Max. Temp	33.36	27.22	36.28
Aver. Temp.	27	22.62	28.61
Δ Temp	15.22	20.84	14.88

To know about the distribution of the data, the information from the surface temperature also explain using a bar chart diagram and the results are shown in Figure 6, Figure 7, and Figure 8. On the graph, the vertical line shows the number of pixels and the horizontal line shows the temperature value.

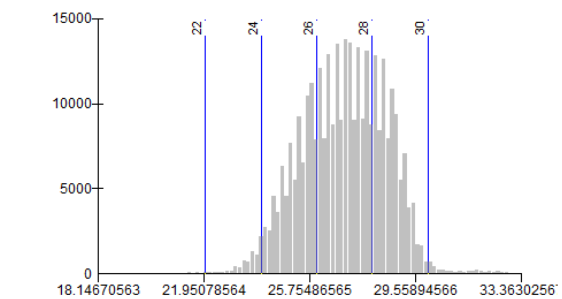


Fig. 6. Temperature distribution data before Covid-19 (August 2019)

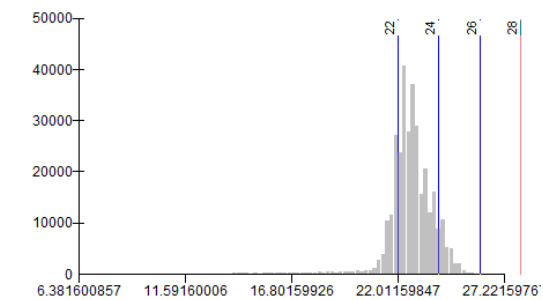


Fig. 7. Temperature distribution data during Covid-19 (May 2020)

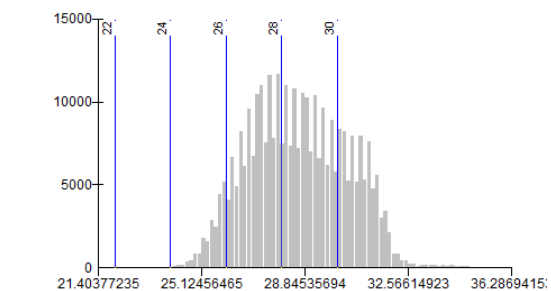


Fig. 8. Temperature distribution data after new normal (August 2020)

Viewed from the perspective of each district in the Yogyakarta urban agglomeration, the Yogyakarta city is the area with the highest temperature in each session. This information shown in Table 4.

Table 4. Comparison of average temperature in each district inside Yogyakarta Urban Agglomeration

District	Before pandemic	During pandemic	After new normal
Yogyakarta City	28.65	23.90	30.95
Sleman	26.88	22.36	28.24
Bantul	26.60	22.62	28.47

The bar chart diagram for table 4 shown in Figure 9. Sleman and Bantul has a slightly different and almost the same temperature value.

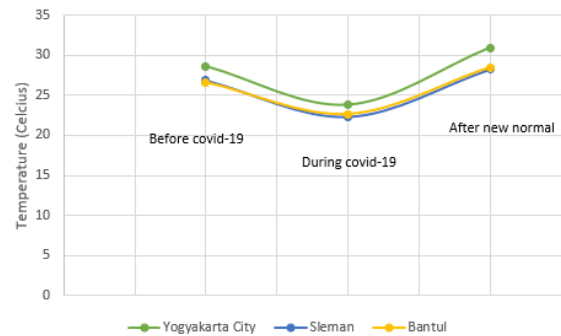


Fig. 9. Temperature graph in each district inside Yogyakarta Urban Agglomeration

A mobility index data released by Google reported in D.I. Yogyakarta from during pandemic (March 01 to June 30, 2020) and after new normal (July 01 to August 31, 2020) in Table 5. The data shows that the mobility of D.I. Yogyakarta decreased during a pandemic for outdoor activity that comprises retail and recreation, grocery and pharmacy, parks and outing, transport, and workplace. For activity in the residential sector is increased. After the new normal, outdoor activity slightly increased from the previous and residential activity a little further down.

Table 5. Mobility index report In D.I. Yogyakarta by google tracking

Category	During pandemic	After new normal
Retail and recreation	-36.48%	-21.52%
Grocery and pharmacy	-23.17%	-15.24%
Parks and outing	-48.44%	-27.85%
Transport	-59.90%	-52.69%
Workplace	-29.62%	-26.37%
Residential	14.58%	11.27%

The table 5 above visualized in graph that shown in Figure 10 for during pandemic and after new normal.

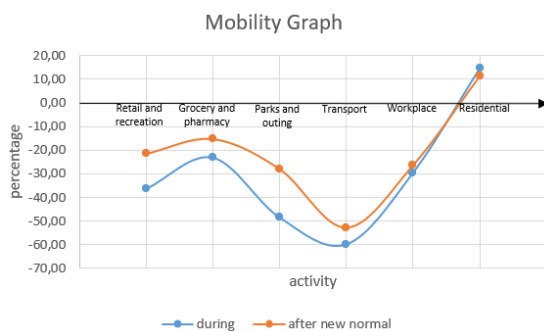


Fig. 10. Mobility graph during pandemic and after new normal

4. Conclusion

The rapid urbanization in Yogyakarta's urban agglomeration increased the temperature level of the area. The rise of temperature at the Yogyakarta urban agglomeration can threaten the environment and around the globe because of global warming. The Covid-19 pandemic influences the atmospheric temperature. The policy for minimizing outdoor activity has been reduced the land surface temperature level. The limitation of outdoor activity due to the Covid-19 pandemic in Yogyakarta urban agglomeration, the temperature level significantly getting better. The land surface temperature tends to decrease compared to before the pandemic. But after the new normal, human activity starts to normal. People can do an outdoor activity with health protocol. This condition triggers the temperature is increased. From satellite imagery processing investigate the temperature level after the new normal is the same as before the pandemic, even a little higher. This concludes that the restriction policy has affected the thermal condition of Yogyakarta's urban agglomeration. Less human outdoor activity during the enforcement of the policy, reducing the land surface temperature.

References

Avdan, U., Jovanovska, G., 2016. Algorithm for automated mapping of land surface temperature using LANDSAT 8 satellite data. *J. Sensors* 2016. doi.org/10.1155/2016/1480307

Bendib, A., Dridi, H., Kalla, M.I., 2017. Contribution of Landsat 8 data for the estimation of land surface temperature in Batna city, Eastern Algeria. *Geocarto Int.* 32, 503–513. doi.org/10.1080/10106049.2016.1156167

Feng, Y., Gao, C., Tong, X., Chen, S., Lei, Z., Wang, J., 2019. Spatial patterns of land surface temperature and their influencing factors: A case study in Suzhou, China. *Remote Sens.* 11. doi.org/10.3390/rs11020182

Kong, W.H., Li, Y., Peng, M.W., Kong, D.G., Yang, X.B., Wang, L., Liu, M.Q., 2020. SARS-CoV-2 detection in patients with influenza-like illness. *Nat. Microbiol.* 5, 675–678. doi.org/10.1038/s41564-020-0713-1

Logan, T.M., Zaitchik, B., Guikema, S., Nisbet, A.,

2020. Night and day: The influence and relative importance of urban characteristics on remotely sensed land surface temperature. *Remote Sens. Environ.* 247, 111861. doi.org/10.1016/j.rse.2020.111861

Maithani, S., Nautiyal, G., Sharma, A., 2020. Investigating the Effect of Lockdown During COVID-19 on Land Surface Temperature: Study of Dehradun City, India. *J. Indian Soc. Remote Sens.* 48, 1297–1311. doi.org/10.1007/s12524-020-01157-w

Mathew, A., Khandelwal, S., Kaul, N., 2016. Spatial and temporal variations of urban heat island effect and the effect of percentage impervious surface area and elevation on land surface temperature: Study of Chandigarh city, India. *Sustain. Cities Soc.* 26, 264–277. doi.org/10.1016/j.scs.2016.06.018

Miles, V., Esau, I., 2017. Seasonal and spatial characteristics of Urban Heat Islands (UHIs) in northern West Siberian cities. *Remote Sens.* 9. doi.org/10.3390/rs9100989

Ndossi, M.I., Avdan, U., 2016. Application of open source coding technologies in the production of Land Surface Temperature (LST) maps from Landsat: A PyQGIS plugin. *Remote Sens.* 8. doi.org/10.3390/rs8050413

Neinavaz, E., Skidmore, A.K., Darvishzadeh, R., 2020. Effects of prediction accuracy of the proportion of vegetation cover on land surface emissivity and temperature using the NDVI threshold method. *Int. J. Appl. Earth Obs. Geoinf.* 85. doi.org/10.1016/j.jag.2019.101984

Pal, S., Ziaul, S., 2017. Detection of land use and land cover change and land surface temperature in English Bazar urban centre. *Egypt. J. Remote Sens. Sp. Sci.* 20, 125–145. doi.org/10.1016/j.ejrs.2016.11.003

Phelan, P.E., Kaloush, K., Miner, M., Golden, J., Phelan, B., Silva, H., Taylor, R.A., 2015. Urban Heat Island: Mechanisms, Implications, and Possible Remedies. *Annu. Rev. Environ. Resour.* 40, 285–307. doi.org/10.1146/annurev-environ-102014-021155

Sahani, N., Goswami, S.K., Saha, A., 2020. The impact of COVID-19 induced lockdown on the changes of air quality and land surface temperature in Kolkata city, India. *Spat. Inf. Res.* doi.org/10.1007/s41324-020-00372-4

Sekertekin, A., Zadbagher, E., 2021. Simulation of future land surface temperature distribution and evaluating surface urban heat island based on impervious surface area. *Ecol. Indic.* 122, 107230. doi.org/10.1016/j.ecolind.2020.107230

Srivastava, N., Hinton, G., Krizhevsky, A., Sutskever, I., Salakhutdinov, R., 2014. Dropout: A Simple Way to Prevent Neural Networks from Overfitting. *J. Mach. Learn. Res.* 15, 1929–1958. doi.org/10.1214/12-AOS1000

Wang, Z., Liu, M., Liu, X., Meng, Y., Zhu, L., Rong,

- Y., 2020. Spatio-temporal evolution of surface urban heat islands in the Chang-Zhu-Tan urban agglomeration. *Phys. Chem. Earth* 117, 102865. doi.org/10.1016/j.pce.2020.102865
- Yu, X., Guo, X., Wu, Z., 2014. Land surface temperature retrieval from landsat 8 TIRS-comparison between radiative transfer equation-based method, split window algorithm and single channel method. *Remote Sens.* 6, 9829–9852. doi.org/10.3390/rs6109829